2014 IEEE International Conference on Fuzzy Systems (FUZZ-IEEE)
July 6-11, 2014, Beijing, China

Optimal Fuzzy Logic Based Coordination Controller for Improved Transient Stability of a Smart Grid

Ganesh Kumar Venayagamoorthy, *Senior Member, IEEE,* and Priyam Chakravarty, *Member, IEEE*

Abstract— **While smart grid disturbances are inevitable, their effects can be minimized through intelligent power management and control. SmartParks (large numbers of electric vehicles capable of performing bidirectional power transactions) or energy storage systems can be used to improve the transient stability of a smart grid with wind farms when faults are experienced. In this paper, the speed oscillations in conventional generators are minimized by optimizing a fuzzy logic controller performing coordinated control between SmartParks and a wind farm. A novel heuristic search based algorithm, mean variance optimization, is applied for the optimization tasks. The results demonstrate the improvement in the overall transient stability of the system operating under disturbances at different locations in the system.**

I. Introduction

THE analysis of disturbances such as grid faults and power fluctuations in power systems has gained importance with recent increases in the use of power electronic devices connected to the grid [1]. Such devices include doubly fed induction generator (DFIG) based wind farms and plug-in electric vehicle parking lots (SmartParks). The sensitivity of these devices causes problems when faults and power deviations occur. In DFIGs, the induction generator is connected to the grid at the stator terminals, but the rotor terminals are connected via a partial-load, variable frequency, AC/DC/AC converter and a transformer [2]. This increases the efficiency of a DFIG because the variable frequency converter (VFC) requires only a fraction of the total power to achieve full control of the generator.

Power fluctuations can be reduced and dynamic performance improved during transient disturbances in DFIGs through decoupled control of the generator's active and reactive power [3]. However, the VFC of a DFIG and its power electronics (IGBT-switches) are highly sensitive to transient disturbances in power networks. When subjected to faults or voltage sags, the rotor-side converter of the VFC might become blocked due to protection from overcurrent in the rotor circuit, and the wind turbine can be tripped from the system [2]. The VFC is controlled by a set of proportional integral (PI) controllers. With optimally designed controllers, the wind generator can withstand transient grid disturbances under a range of different wind speed conditions.

However, wind energy is variable in nature. If the wind speed is low, the maximum possible power is extracted from the wind turbine corresponding to that wind speed. If the wind speed is high, the pitch control actively limits the power generated from the wind turbine. This kind of power generation fluctuation in a wind farm connected to the grid may cause stability problems in the system. To solve this problem, the use of plug-in vehicle parking lots (SmartParks) for energy storage was proposed in [4]. The number of plug-in electric vehicles (PEVs) entering the market is increasing, and many of these vehicles are expected to participate in vehicle-to-grid (V2G) power transactions in the proposed smart grid infrastructure, where bidirectional power flow between the vehicle and the grid will become essential [5-6]. The use of SmartParks connected to the grid as energy storage mechanisms is proposed in [7] as a way to minimize the shock on the system due to wind gusts, reduce congestion in the transmission lines, and improve the stability of the system during rapid fluctuations in wind speed [7].

A smart electric power grid consisting of a wind farm and multiple distributed SmartParks was presented in [4]. Investigations showed that it was necessary to retune the PI controllers as the wind speed changed and different grid disturbances occurred, despite the presence of energy storage. A practical power system should be capable of withstanding grid faults over a range of varying wind speeds. In order to achieve this goal, it is critical to tune the PI controllers of the rotor side converter (RSC) of the VFC. This study proposes a new stochastic optimization technique called the mean variance optimization (MVO) algorithm [8] to perform online tuning of controllers based on wind farm operating under variable wind speed conditions and grid disturbances.

SmartParks can only be coordinated with wind farms using a proper control strategy. A fuzzy logic [9] based controller was proposed in [10] that uses the difference between the demand and availability of wind power and the overall state-of-charge of the SmartParks as inputs, and, according to certain rules, generates the charging or discharging power commands for the SmartParks and the pitch control reference of the wind farm. In this paper, a novel optimization method, mean-variance optimization (MVO), is applied to evolve an optimal fuzzy logic controller. The membership functions of the fuzzy logic controller are optimized in order to improve the transient stability of the smart grid by minimizing the oscillations in the wind farm output and the speed deviations of conventional generators in

G. K. Venayagamoorthy is with the Real-Time Power and Intelligent Systems Laboratory, Clemson University, SC 29634, USA (corresponding author phone: 864-656-5936; fax: 864-656-1411; e-mail: gkumar@ieee.org).
P. Chakravarty is with the Structure Group, Houston, TX, USA (priyam.chakravarty@thestructuregroup.com).
The support for this study from the US National Science Foundation under the following grants is gratefully acknowledged by the authors: NSF EFRI # 1238097, GOALI–ECCS # 0802047 and IIP 1312260.

the grid under the influence of grid faults at different locations.

II. Modeling Of The Test System

The smart grid test system includes a DFIG based wind farm and SmartParks (Fig. 1). The system has two other synchronous generators, an infinite bus, and three interconnected areas. The parameters of this system are given in [11]. A typical city will have several SmartParks distributed throughout at distances of one to a few miles. In order to represent this design, six three-phase PEV parking lots (PL1 to PL6 – 120 MW) are added to Area 2 of this system at bus 13, which is an additional bus added to the original 12-bus system [11] in order to connect the PEV SmartParks. Bus 13 is connected to bus 6 through 22 kV/230 kV step-up transformers. The smart grid test system (Fig. 1) is implemented on a real-time digital simulator (RTDS) [12].

In this study, a 400 MW wind farm is modeled using a single DFIG. It uses back-to-back PWM converters for variable-speed wind power generation. The control objective of the grid-side converter is to keep the dc link voltage constant regardless of the magnitude and direction of the rotor power [3]. A stator-oriented vector control approach is used in which the direct axis current controls the dc link voltage and the quadrature axis current controls the reactive power and, in turn, the voltage at the point of common coupling. The objective of the RSC is to control the active and reactive power from the stator, which it achieves by positioning the d-axis of the rotor reference frame along the stator flux vector. The q-axis current reference is generated directly from the commanded electrical power, and the d-axis current reference is generated from the stator reactive power command. The electrical power command is generated from the optimum operating point tracking strategy, when the wind speed is below a certain value. The pitch control does not work at that time, and the wind turbine captures the maximum possible power at the available wind speed. However, if the wind speed exceeds a certain value, the pitch control limits the power generated by the wind turbine. Fig. 2 shows the rotor-side and grid-side converter control strategy.

The SmartPark model in this paper is represented by a battery followed by a bidirectional, three-phase inverter (Fig. 3) [13]. The inverter generates a 2.08 kV, three-phase, line-to-line rms voltage, which passes through a 2.08kV/22kV step-up transformer and is connected to the SmartPark bus (bus-13 in Fig. 1). Between the inverter and the transformer is a small (0.5mH) inductance. The control of the inverters is designed in such a way that each inverter can draw ±20 MW of active power. Considering that each vehicle can draw ±25 kW, each SmartPark in this paper represents 800 aggregated vehicles. Here, the '+' sign indicates that the vehicles are selling power to the grid, i.e., they are in discharging mode, and the '-' sign indicates that they are buying power from the grid, i.e., they are in charging mode. Fig. 4 depicts the control strategy for the PEV. In the d-q reference frame, the active and reactive powers coming out of the inverter are [14]:

$$P = (3/2)\cdot(v_{qs}i_{qs} + v_{ds}i_{ds}) \tag{1}$$

$$Q = (3/2)\cdot(v_{qs}i_{ds} + v_{ds}i_{qs}) \tag{2}$$

In the synchronous reference frame, the peak line-to-neutral voltage is in the q-axis, and $v_{ds} = 0$. Therefore, the basis of the control is to command the currents in response to the demanded power:

$$i_{qs}^{*} = (2/3\sqrt{2})\cdot(P^{*}/v_{peak}) + (K_i/s)\cdot(P^{*} - P) \tag{3}$$

$$i_{ds}^{*} = (2/3\sqrt{2})\cdot(Q^{*}/v_{peak}) + (K_i/s)\cdot(Q^{*} - Q) \tag{4}$$

The first component of (3) and (4) is based on the power equations given in (1) and (2), where v_{peak} is a filtered version of the line-to-neutral rms voltage. This component creates a fast response to sudden changes in the commanded power. The integral term trims out the steady-state error. As shown in Fig. 3, a limit is placed on the commanded current to prevent integrator windup. The commanded q- and d-axis currents then are transformed to a-b-c variables, where delta current regulation is used to control the converter transistor switches.

III. Mean-Variance Optimization Algorithm

The MVO algorithm depicted in Fig. 5 is a new population-based stochastic optimization technique introduced in [7]. The mapping function transforms the uniformly distributed random variation into a population attained so far. The MVO algorithm, which finds the near-optimal solution, is simple to implement, requiring only one fitness evaluation per iteration regardless of the number of individuals in the population.

In many other heuristic algorithms, this is not the case. The number of fitness evaluations is proportional to the number of individuals/particles/chromosomes in the population. Fitness evaluation is the most time-consuming task in tuning using heuristic approaches. Fewer fitness evaluations are preferred for fast, online tuning of PI controllers. The MVO algorithm is therefore a very attractive and computationally efficient algorithm for online controller tuning.

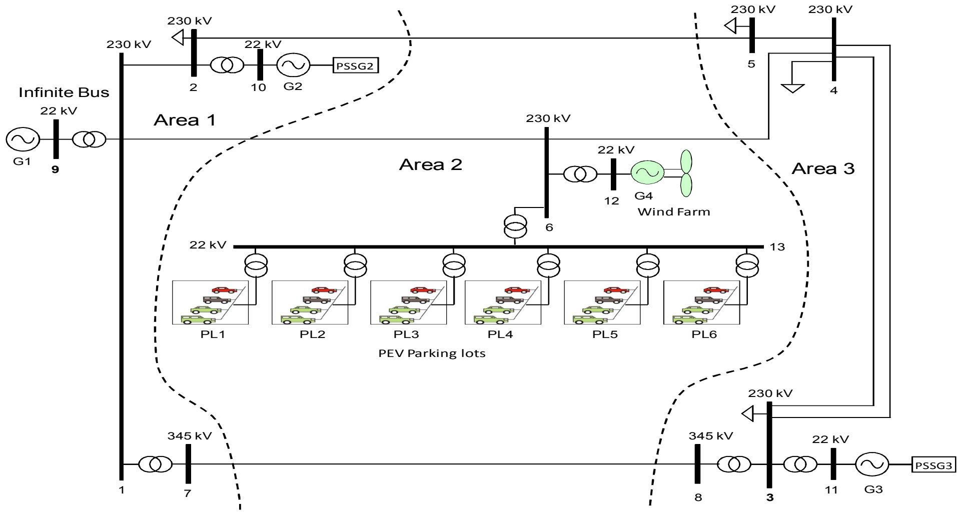

Fig. 1.Smart grid model consisting of a transmission network with a wind farm (400 MW) and large distributed SmartParks (120 MW). The rest of the parameters of the system are given in [11].

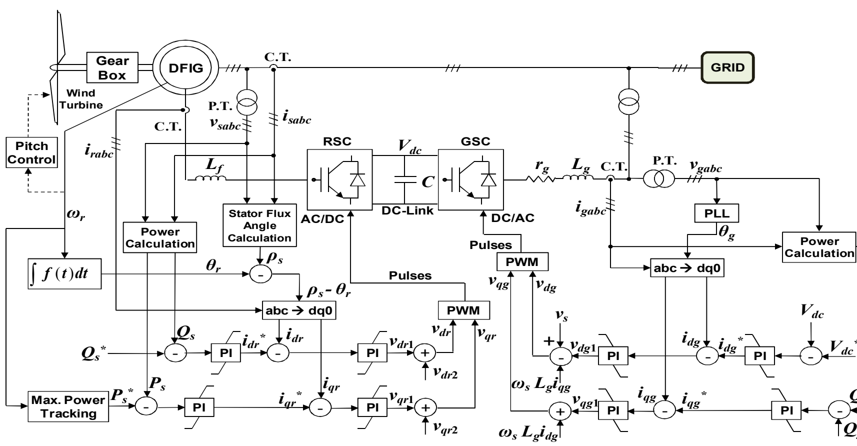

Fig. 2.Rotor- and stator-side controls of the DFIG based wind farm.

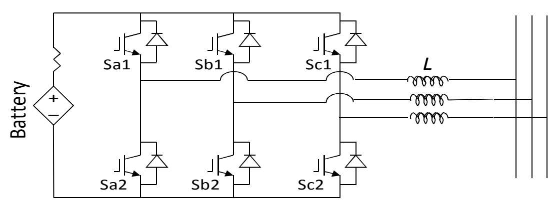

Fig. 3. Dc voltage source (battery) followed by the inverter.

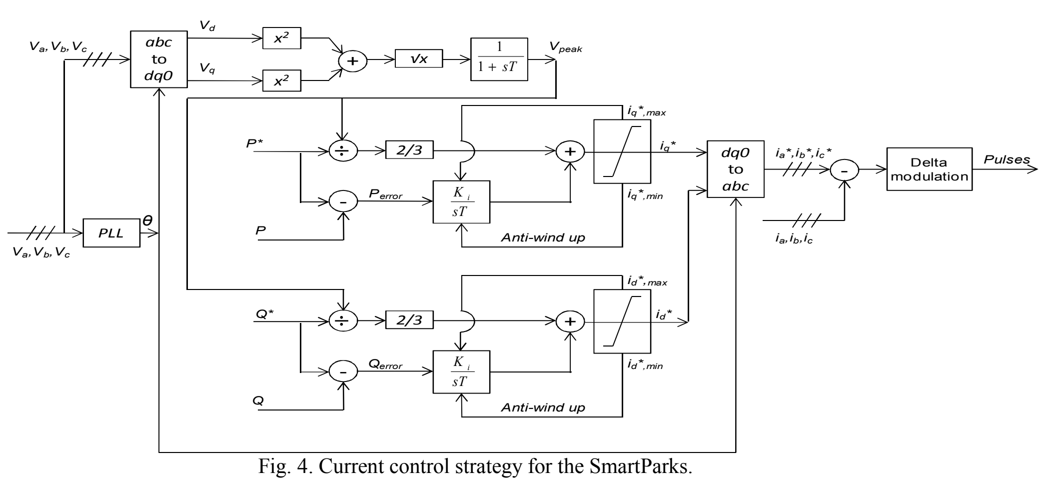

Fig. 4. Current control strategy for the SmartParks.

MVO requires a small population compared to other search based algorithms, such as Particle Swarm Optimization (PSO). The dimension of optimization is the number of parameters to be tuned. The fitness of the MVO is a performance index used to evaluate the system's performance. The goal of the MVO is to maximize or minimize the fitness by changing the system parameters, which are limited by system constraints. The MVO also involves termination criteria, which means that it has a maximum number of allowed iterations. In [8], three selection criteria were proposed for selecting the dimensions to be mutated. The study described in the current paper employs random selection of one of six dimensions. Only one dimension at a time is selected for mutation because optimization is carried out online, and extreme changes in controller behavior could initiate system instability. The selected dimension is mutated using the process illustrated in Fig. 5. Finally, the best dimensions or system parameters are copied into the remaining dimensions so as to create a new offspring.

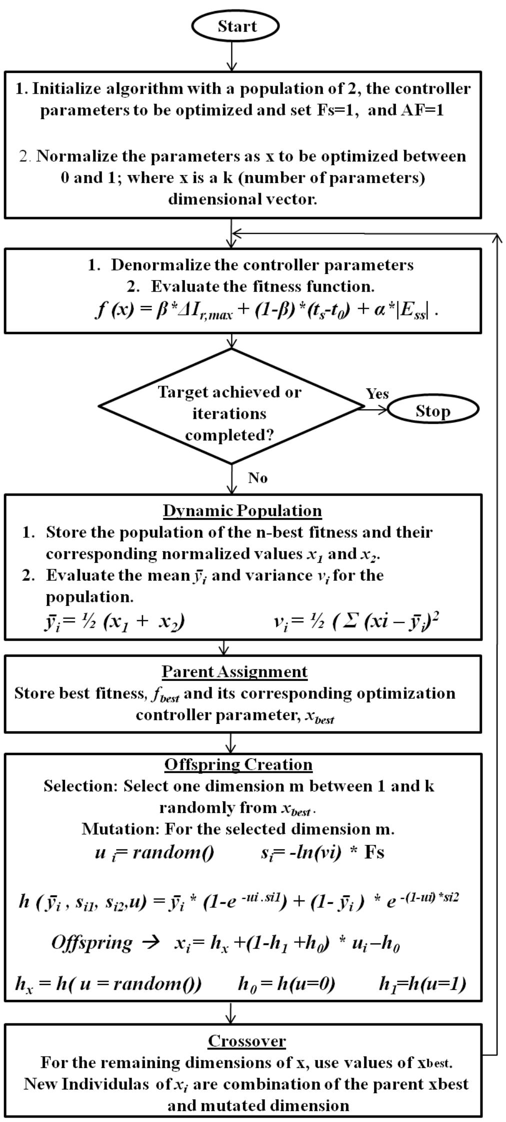

Fig. 5. Mean variance optimization flowchart for PI controller tuning.

IV. Development Of Optimal Fuzzy Logic Controller

Fuzzy logic is the logic underlying approximate, rather than exact, modes of reasoning [9]. Fuzzy logic controllers are based on a set of if-then rules that are developed based on experiential data. For example, if the difference between the available wind power and the demand is *negative big* and the overall state of charge is *medium*, then the SmartPark power command is *positive (discharging) big* and the pitch control reference is *very high*.

Therefore, the inputs to the fuzzy logic controller form membership functions based on the if-then rules. A Sugeno fuzzy logic controller was proposed in [7]. This controller has triangular membership functions between which the entire range of inputs/outputs is distributed. The goal of the fuzzy logic controller (FLC) is to use the SmartParks for energy storage to reduce the shock on the system when there is a fault. Moreover, with an energy storage device, the wind power generation limit imposed by the pitch control during a wind gust can be increased, thus yielding a more optimal utilization of the wind energy.

The maximum possible amount of charging and discharging by the parking lots will depend on the state of charge of the batteries of the plug-in vehicles present at those parking lots at that particular moment. Therefore, the aggregated state of charge of the parking lots and the wind power demand must be monitored continuously when using this control strategy. The wind power demand is compared with the actual wind power generated by the wind farm at that instant, and the difference is used as one of the inputs to the fuzzy controller. Based on these two inputs, the controller outputs the charging and discharging commands for the SmartParks, as well as the pitch angle reference for the wind farm. Fig. 6 shows the schematic diagram of the coordinated controller. Due to the nonlinearity in the relationships among these variables, it is very difficult to design a classical controller for this kind of coordinated control. A fuzzy logic controller is suitable for this purpose because it allows a set of rules to be derived that relate the variables using experiential knowledge.

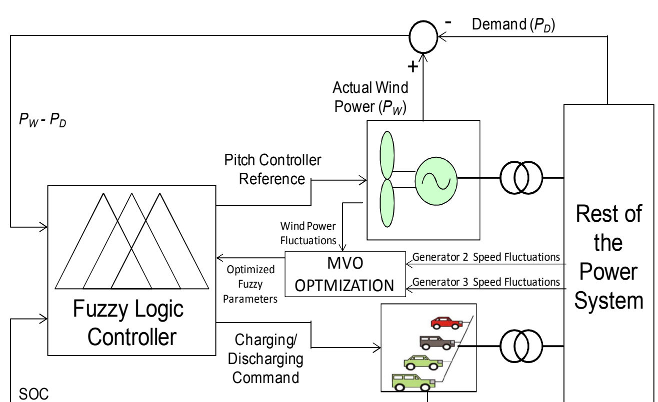

Fig. 6. Optimized fuzzy logic based coordination controller.

There are two inputs to the fuzzy logic controller:

- Difference between Wind Power Available (P_W) and

Instantaneous Power Demand (P_D): This input parameter varies from -250 MW to 250 MW. This range is distributed between five membership functions: NB (Negative Big), NS (Negative Small), Z (Zero), PS (Positive Small), and PB (Positive Big). The initial spacing is equal for each function (Fig. 7). However, MVO will be implemented to optimize the spacing of the membership function.

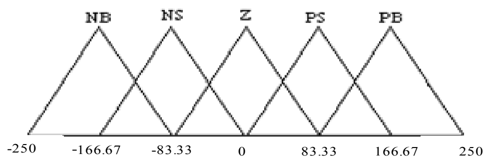

Fig. 7. Membership function of first input (P_W-P_D)

- State of Charge of SmartParks (SOC): The SOC of the SmartParks varies between 20% and 80%. This range is distributed between seven membership functions: Very Low (VL), Low (L), Medium Low (ML), Medium (M), Medium High (MH), High (H), and Very High (VH). The initial spacing is equal for each function (Fig. 8).

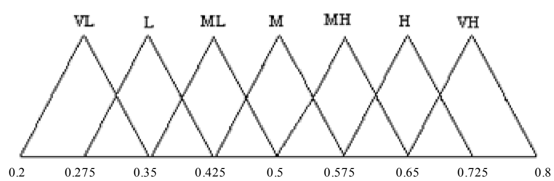

Fig. 8. Membership function of second input (SOC)

There are two outputs from the fuzzy logic controller:

- Pitch Controller Reference: This output parameter varies within the narrow range of 1.15 to 1.25. This range is distributed between seven membership functions: Very Low (VL), Low (L), Medium Low (ML), Medium (M), Medium High (MH), High (H), and Very High (VH). The initial spacing is equal for each function. However, MVO will be implemented to optimize the spacing of the membership function depicted in Fig. 9.

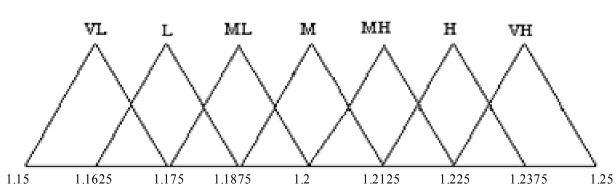

Fig. 9. Membership function of first output (pitch controller reference).

- Power Command of SmartParks: The power command of the SmartParks varies between +/- 120 MW. This range is distributed between seven membership functions: NB (Negative Big), NM (Negative Medium), NS (Negative Small), Z (Zero), PS (Positive Small), PM (Positive Medium), and PB (Positive Big). The initial spacing for the Sugeno membership function is equal (Fig. 10).

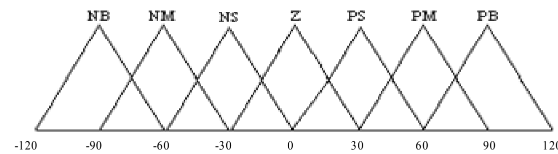

Fig. 10. Membership function of second output (power command of SmartParks).

Tables I and II contain the rule bases for the two outputs. The rules generate the weights for each output's firing strength, and the final outputs are calculated using the center-of-area method.

TABLE I
RULE BASE FOR PITCH CONTROLLER REFERENCE

SOC	P_W - P_D				
	NB	NS	Z	PS	PB
VL	VH	VH	VH	VH	VH
L	VH	VH	VH	VH	H
ML	VH	VH	VH	H	MH
M	VH	VH	VH	H	M
MH	VH	VH	H	MH	ML
H	VH	VH	MH	M	L
VH	VH	H	M	L	VL

TABLE II
RULE BASE FOR POWER COMMANDS TO THE SMARTPARKS

SOC	P_W - P_D				
	NB	NS	Z	PS	PB
VL	PB	PS	Z	NB	NB
L	PB	PS	Z	NB	NB
ML	PB	PM	Z	NB	NB
M	PB	PB	Z	NB	NB
MH	PB	PB	Z	NM	NB
H	PB	PB	Z	NS	NB
VH	PB	PB	Z	NS	NB

Fuzzy logic controllers can be improved further by optimizing the membership functions. MVO is used for this purpose. The following steps are followed to implement the MVO algorithm for developing optimal fuzzy logic parameters:

i. Population: A population of two is used, similar to [8].
ii. Dimension: The FLC consists of two inputs, one with seven parameters and one with nine parameters. The FLC also has two outputs with nine parameters each. Therefore, 34 parameters require optimization, which becomes the dimension of optimization.
iii. Fitness function: The goal of the MVO is to find the optimal parameters for the FLC by minimizing a fitness function. Optimization is carried out in order to minimize fluctuations in the generation speed of generator 2 (ω_2) and the generator speed of generator 3 (ω_3) (Fig. 1). The following fitness function is used to

evaluate the system's transient response, where f_1 and f_2 are the wind power fluctuations, speed of generator 2, and speed of generator 3, respectively:

$$f_1 = \beta_2 * \Delta\ \omega_{2,max} + (1-\beta_2)*(t_{s2}-t_{02}) + \alpha_2 * |E_{ss2}| \qquad (5)$$

$$f_2 = \beta_3 * \Delta\ \omega_{3,max} + (1-\beta_3)*(t_{s3}-t_{03}) + \alpha_3 * |E_{ss3}| \qquad (6)$$

where $\Delta P_{wind,max}$, $\Delta\ \omega_{1,max,}$ and $\Delta\ \omega_{3,max}$ are the overshoot wind power, overshoot generator 2 speed, and overshoot generator 3 speed; $(t_{s2}-t_{02})$ and $(t_{s3}-t_{03})$ represent the settling time, and E_{ss2} and E_{ss3} stand for the steady state error. β_2, β_3, $\alpha 2$ and α_3 are the weighting factors used to satisfy different design requirements. A cumulative fitness (U_{total}) was computed as in (7), where k_1 and k_2 are the weighting constants for the terms f_1, f_2 and f_3, respectively.

$$U_{total} = k_1 . f_1 + k_2 . f_2 \qquad (7)$$

iv. Limitations: The parameters of the FLC are allowed to vary between the specified limitations of the system. The difference between wind power available (P_W) and instantaneous power demand varies by ±250 MW. The SOC of the SmartParks varies between 20% and 80%. The range of the pitch reference parameter varies within a narrow range of 1.15 to 1.25. Finally, the power command parameter of the SmartParks varies between ±120 MW.

v. Termination criterion: A maximum of 6000 MVO iterations is allowed.

vi. Selection criteria: One of 34 dimensions is randomly selected. Only one dimension is selected for mutation at a time because optimization is carried out online, and extreme changes in controller behavior could initiate system instability.

vii. Mutation and crossover are carried out using the formulas from the flowchart depicted in Fig. 10.

V. RESULTS

The goal of the fuzzy logic controller optimization was to reduce oscillations in the generation speed of G2 (ω_2) and the generator speed of G3 (ω_3). The convergence of MVO was very rapid over the first 500 iterations and then gradually slowed until the best parameters were obtained at the 1895th iteration. The initial parameters of the FLC were equally distributed over the range of the parameters, as shown in Figs. 7-10. These parameters then were optimized with the final membership functions of the inputs and outputs of the FLC, as shown in Fig. 11. For the optimization, $k1$ and $k2$ in (7) were set as 5 and 3, respectively.

In order to demonstrate the effectiveness of the optimal fuzzy logic controllers, three case studies are presented to compare the transient stability of the system when faults are introduced at different locations in the smart grid.

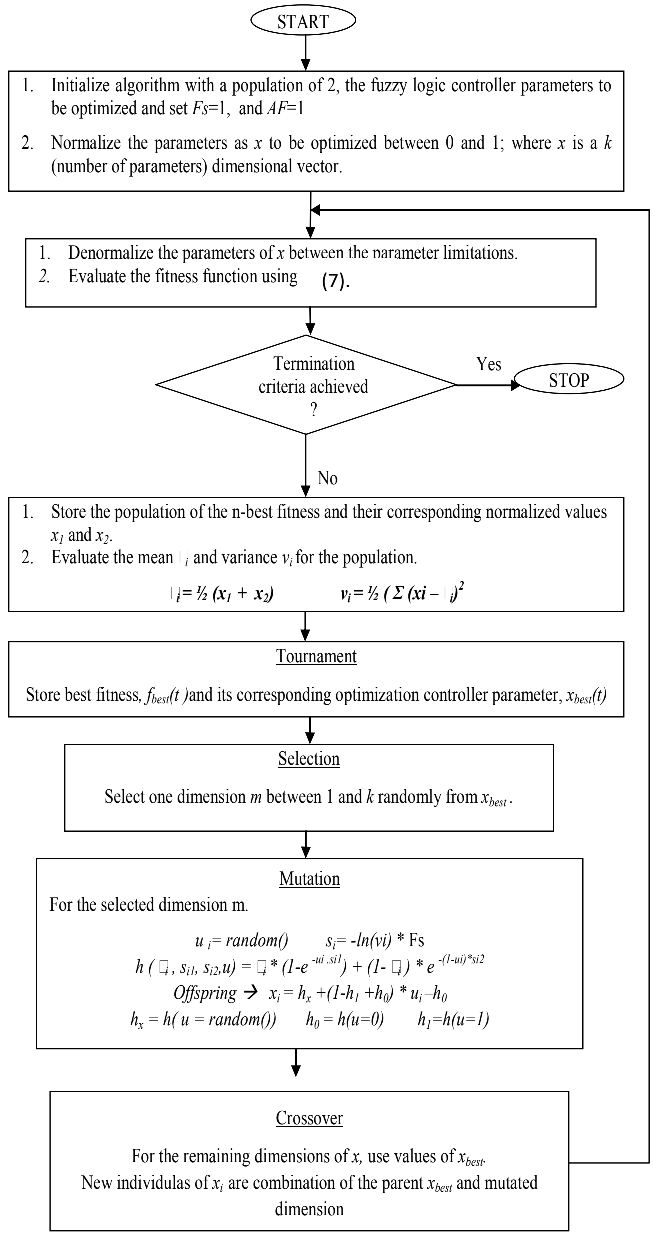

Fig.10. Mean variance optimization flowchart for FLC tuning

Case I: Three-phase short circuit at bus 5: A six-cycle (100 ms) temporary three-phase short circuit fault is applied at bus 5. Fig. 12 compares the power fluctuations in the generator speeds of the two conventional generators without a fuzzy logic controller, with a fuzzy logic controller, and with an optimal fuzzy logic controller. The fault is closer to generator G2, so higher oscillations occur in that generator's speed (ω_2) (Fig. 12.a). The fuzzy logic controller improves the transient responses of both generator G2 and generator G3. Table III shows the damping ratios obtained due to the fault at the two generators, and the improvement that optimization yielded is clear.

Case II: Three-phase short circuit at bus 4: A six-cycle (100 ms) temporary three-phase short circuit fault is applied at bus 5, which is closer to generator G3, with a wind farm operating at 11m/s. This signifies greater oscillations in the generator 3 machine speed (ω_3). Results similar to those in Case I are obtained, as illustrated in Fig. 13. The oscillation of both generators improves due to the optimized fuzzy logic controllers. The Prony analysis in Table IV shows that the damping increases with an optimized fuzzy logic controller; hence, the system achieves better transient stability as a result of the optimization.

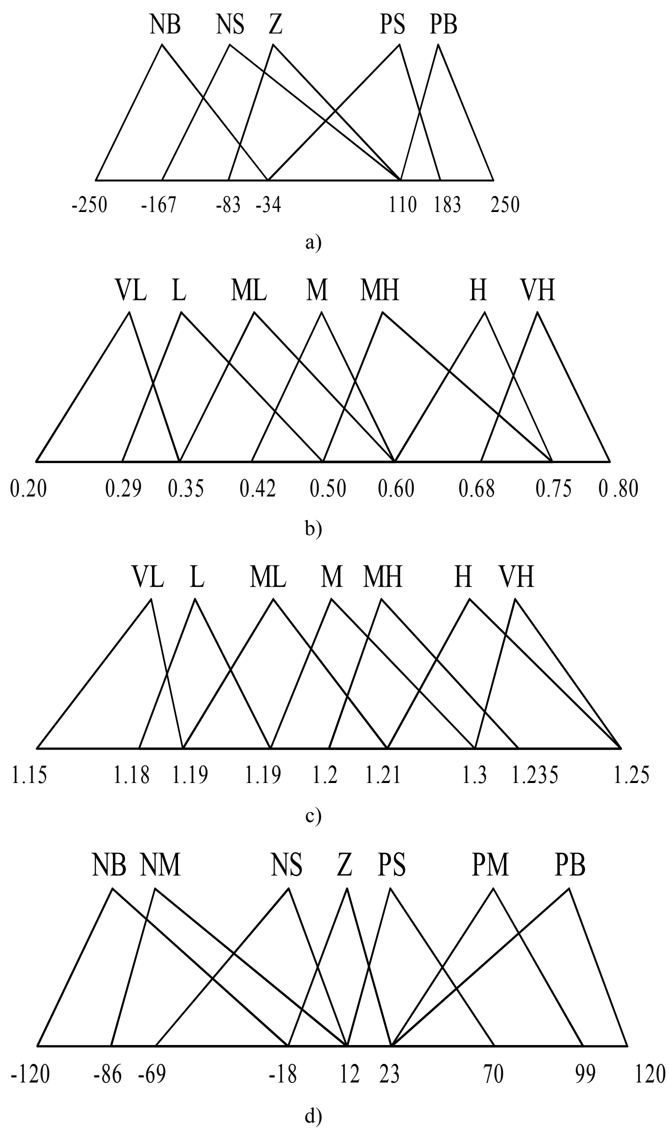

Fig. 11 a) Optimized membership function of first input (P_W-P_D); b) Optimized membership function of second input (SOC); c) Optimized membership function of first output (pitch controller reference); d) Optimized membership function of second output (power command of SmartParks).

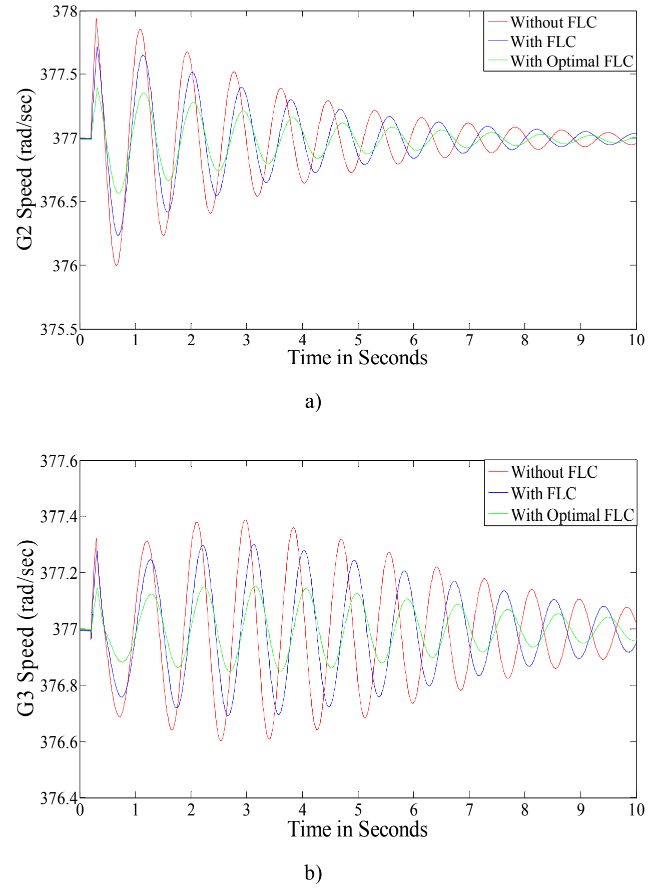

Fig. 12. a) Comparison of machine speed (rad/sec) of generator 2 in the smart grid without FLC, with FLC, and with optimal FLC for a 6-cycle (100 ms), three-phase, line-ground fault applied at bus 5; b) Comparison of machine speed (rad/sec) of generator 3 in the smart grid without FLC, with FLC, and with optimal FLC for a 6-cycle (100 ms), three-phase, line-ground fault applied at bus 5.

TABLE III
NATURAL FREQUENCIES (Ω_N) AND DAMPING RATIOS (Z) OBTAINED FROM PRONY ANALYSIS OF THE GENERATOR SPEEDS WITH A GRID FAULT AT BUS 5

	Without FLC		With FLC		With Optimal FLC	
	ω_N	ζ	ω_N	ζ	ω_N	Z
G2	0.758	0.042	0.759	0.042	0.715	0.067
	1.515	0.037	1.439	0.039	1.487	0.051
G3	0.729	0.030	0.740	0.054	0.736	0.095
	1.487	0.021	1.511	0.033	1.479	0.058

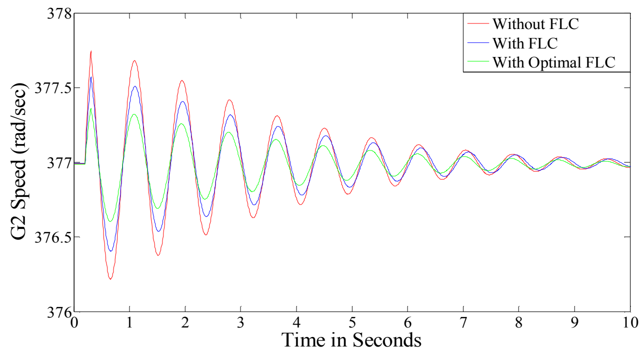

a)

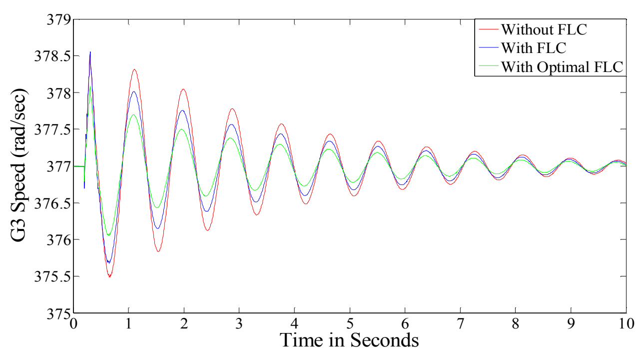

b)

Fig. 13.a) Comparison of machine speed (rad/sec) of generator 2 in the smart grid without FLC, with FLC, and with Optimal FLC for a 6-cycle (100 ms), three-phase, line-ground fault applied at bus 4; b) Comparison of machine speed (rad/sec) of generator 3 in the smart grid without FLC, with FLC, and with optimal FLC for a 6-cycle (100 ms), three-phase, line-ground fault applied at bus 4.

TABLE IV
NATURAL FREQUENCIES (ω_N) AND DAMPING RATIOS (ζ) OBTAINED FROM PRONY ANALYSIS OF THE GENERATOR SPEEDS WITH A GRID FAULT AT BUS 4

	Without FLC		With FLC		With Optimal FLC	
	ω_N	ζ	ω_N	ζ	ω_N	ζ
G2	0.754	0.043	0.791	0.054	0.781	0.079
	1.501	0.028	1.517	0.044	1.521	0.059
G3	0.739	0.103	0.728	0.134	0.711	0.180
	1.437	0.031	1.461	0.064	1.471	0.083

VI. Conclusion

An intelligent and efficient technique for learning the optimal fuzzy logic controller for a smart grid control application has been presented. A novel heuristic mean-variance optimization algorithm was applied to enhance the performance of the fuzzy controller. The proposed coordination controller can reduce the shock in the system and also improve the stability of the system. The performance of both the optimized and un-optimized fuzzy controllers was demonstrated with different case studies, and their effectiveness as a shock absorber was compared with a system having no such coordinated control. The results demonstrate that the optimization improved the overall transient stability of the system operating under faults at different buses.

References

[1] D. Granados Lieberman, R.J. Romero-Troncoso, R.A. Osornio-Rios, A. Garcia-Perez, and E. Cabal-Yepez , "Techniques and Methodologies for Power Quality Analysis and Disturbances Classification in Power Systems: A Review," Generation, Transmission & Distribution, IET, vol. 5, no. 4, pp. 519-529, April 2011.

[2] W. Qiao, G. K. Venayagamoorthy, and R. G. Harley, "Design of Optimal PI Controllers for Doubly Fed Induction Generators Driven by Wind Turbines Using Particle Swarm Optimization," 2006 International Joint Conference on Neural Networks, Vancouver, BC, Canada, pp. 1982-1987, July 16 -21, 2006.

[3] R. Pena, J. C. Clare, and G. M. Asher, "Doubly Fed Induction Generator Using Back-to-Back PWM Converter and its Application to Variable-Speed Wind-Energy Generation," IEEE Proceedings. Electric Power Applications, vol. 143, no. 3, pp. 231-241, May 1996.

[4] P. Mitra, G. K. Venayagamoorthy, and K. Corzine, "SmartPark as a Virtual STATCOM," IEEE Transactions on Smart Grid, vol. 2, issue 3, September 2011, pp. 445-455.

[5] W. Kempton and J. Tomić, "Vehicle-to-Grid Power Fundamentals: Calculating Capacity and Net Revenue," Journal of Power Sources, vol. 166, issue 2, 15 April 2007, pp. 549-566.

[6] Y. Saber and G. K. Venayagamoorthy, "Intelligent Unit Commitment with Vehicle-to-Grid – A Cost-Emission Optimization," Journal of Power Sources, vol. 195, issue 3, Feb. 2010, pp. 898-911.

[7] G. K. Venayagamoorthy and P. Mitra, "SmartPark Shock Absorbers for Wind Farms," IEEE Transactions on Energy Conversion, vol. 26, issue 3, September 2011, pp. 990-992.

[8] I. Erlich, G. K. Venayagamoorthy, and N. Worawat, "A Mean-Variance Optimization Algorithm," WCCI 2010 IEEE World Congress on Computational Intelligence, CCIB, Barcelona, Spain, pp. 1-6, July 18-23, 2010.

[9] L. A. Zadeh, "Fuzzy logic," Computer, vol. 21, no. 4, pp. 83-93, April 1988.

[10] P. Mitra and G. K. Venayagamoorthy, "Intelligent Coordinated Control of a Wind Farm and Distributed SmartParks," IEEE Industry Application Society Annual Meeting, Houston, TX, USA, pp. 1-8, October 3 - 7, 2010.

[11] S. Jiang, U. D. Annakkage, and A. M. Gole, "A Platform for Validation of FACTS Models," IEEE Trans. Power Delivery, vol. 21, Jan. 2006, pp. 484–491.

[12] P. Forsyth, T. Maguire, and R. Kuffel, "Real Time Digital Simulation for Control and Protection System Testing," Power Electronics Specialists Conference, Aachen, Germany, vol. 1, pp. 329- 335, June 20-25, 2004.

[13] P. Mitra, G. K. Venayagamoorthy, and K. Corzine, "Real-Time Study of a Current Controlled Plug-in Vehicle for Vehicle-to-Grid Transactions," International Power Electronics Conference IPEC-Sapporo2010, June 21-24, 2010.

[14] P.C. Krause, O. Wasynczuk, and S.D. Sudhoff, *Analysis of Electric Machinery and Drive Systems*, IEEE Press, 2002.

[15] J. Hauer, C. Demeure, and L. Scharf, "Initial Results in Prony Analysis of Power System Response Signals," IEEE Transactions on Power Systems, vol. 5, no. 1, pp. 80–89, 1990.